International Journal of Engineering, Mathematical and Physical Sciences
ISSN: 2517-9934
Vol:13, No:12, 2019

Creation of $Ga_xCo_{1-x}ZnSe_{0.4}$ (x = 0.1, 0.3, 0.5) Nanoparticles Using Pulse Laser Ablation Method

Yong Pan, Li Wang, Xue Qiong Su, Dong Wen Gao

***Abstract*—**To date, nanomaterials have received extensive attention over the years because of their wide application. Various nanomaterials such as nanoparticles, nanowire, nanoring, nanostars and other nanostructures have begun to be systematically studied. The preparation of these materials by chemical methods is not only costly, but also has a long cycle and high toxicity. At the same time, preparation of nanoparticles of multi-doped composites has been limited due to the special structure of the materials. In order to prepare multi-doped composites with the same structure as macro-materials and simplify the preparation method, the $Ga_xCo_{1-x}ZnSe_{0.4}$ (x = 0.1, 0.3, 0.5) nanoparticles are prepared by Pulse Laser Ablation (PLA) method. The particle component and structure are systematically investigated by X-ray diffraction (XRD) and Raman spectra, which show that the success of our preparation and the same concentration between nanoparticles (NPs) and target. Morphology of the NPs characterized by Transmission Electron Microscopy (TEM) indicates the circular-shaped particles in preparation. Fluorescence properties are reflected by PL spectra, which demonstrate the best performance in concentration of $Ga_{0.3}Co_{0.3}ZnSe_{0.4}$. Therefore, all the results suggest that PLA is promising to prepare the multi-NPs since it can modulate performance of NPs.

***Keywords*—**PLA, physics, nanoparticles, multi-doped.

I. Introduction

NANOMATERIAL and nanotechnology have been become the core material technology at present as the development of science [1]. Among the various nanomaterials, the NPs have been extensively used in medical diagnosis, sensing detection, biological exploration, optical device, semiconductor and so on [2]-[4]. Thus, the performance of NPs is the key to their application and research. Now, the preparation methods of NPs mainly include chemical (gas-phase and liquid-phase reaction) and physical (dry or wet crushing, evaporation and sputtering) [5]-[7]. But there are still exist four challenges in those methods including preparation efficiency, irregular shape, the problem of particle clusters and inconsistent components. PLA is a physical process of preparing nanomaterials by bombarding materials from the surface of bulk target with nanosecond, picosecond or femtosecond pulsed laser [8].

Transition metal elements, such as Co, Ni, Fe, Mn, Cr, Cu, Zn, etc., have attracted considerable attention because of their unfilled valence layer orbits, which are quite different from other elements in nature [9], [10]. Among them, Co as a transition metal doping ion is recognized due to its abundant photon transitions energy levels and proven room temperature ferromagnetic property [11]. Ga is very suitable to emit or stimulate the light in range from ultraviolet to visible. Its optoelectronic performance has long attracted people's attention [12]. However, there are still few NP materials that combine these two materials with their superior properties because their composition and content are hard to guarantee.

To solve the problems mentioned above, we adopt the PLA method to fabricate multi-doping materials $Ga_xCo_{1-x}ZnSe_{0.4}$ (x = 0.1, 0.3, 0.5). Regular round NPs are obtained. What is important, we obtained multi-doped composite nanomaterials with unchanged composition. The analysis of the material properties was characterized by a structure, morphology and optical measurement.

II. Experiment

Three concentration ratios with $Ga_xCo_{0.6-x}ZnSe_{0.4}$ (x = 0.1, 0.3 and 0.5) targets were fabricated before thin film. Weighing is the first step of target preparation from powder stock. The quality of powder is directly related to the quality of target preparation, whether the concentration of each component is accurate or not. An analytical electronic scale is an indispensable and important instrument in quantitative analysis. The electronic scale with a precision of 0.1 mg is adopted in this procedure. After weighing, the powder stock will be ground in agate mortar firstly. Agate is a valuable mineral, and its main chemical component is silica. It cannot react with many elements, so it is widely used for grinding various substances. The first manual grinding will take 2 hours in the agate mortar. Then, the powder will be entered in the ball mill device to mechanically grind for about 6 h. The aim of prepressing targets is to mix different powders and to ensure uniformity of sintered targets. The last step of the first process is pre-sintering. The purpose of pre-sintering is to carry out solid phase reaction and to reduce the shrinkage of target sintered after pressing. Furthermore, the pre-burned material is more grinding and refining, so as to promote the reaction completely, make the reaction uniform, and lay a good foundation for the secondary pressure. Thus, the powder is prepared by manually ground for 2 h in an agate mortar, and mechanically ball-milled for about 6 h again.

All of the thin films in this work were synthesized through the method of Pulse Laser Deposition (PLD). The PLD system schematic diagram for this work is shown in Fig. 2. All films were prepared under two different conditions, including 25 ℃-2 Pa and 700 ℃-10 Pa. For the first condition, the vacuum degree of the cavity was pumped to 3.3×10^{-4} Pa by mechanical and molecular pump. In the process of deposition, the pressure of the cavity was adjusted to low pressure of 2.1 Pa, and the

Yong Pan, Li Wang, Xue Qiong Su, ad DongWen Gao are with the College of Applied Sciences, Beijing University of Technology, Beijing, 100124, China (e-mail: panyong_paper@126.com, lwang.1@bjut.edu.cn, nysxq@bjut.edu.cn, 781435901@qq.com).

temperature was maintained at normal temperature of 25 ℃. The laser power was set to a 400 mW of Q-switch pulse, and the deposition time was controlled at 30 min. Besides, for the condition of the high temperature and pressure, the vacuum can only was pumped to 2.3×10^{-3} Pa because of the influence of the high temperature and pressure. Before deposition, the pressure inside the chamber was adjusted to 10 Pa through Ar gas. The flow of Ar gas was 22.0 standard-state cubic centimeter per minute (SCCM). The substrate temperature was raised to 800 ℃, using a substrate heating device installed in the chamber.

The structure of NPs was characterized by XRD technique (Bruker D8 Advance), and Raman spectrum (Horiba Jobin Yvon T6400). The morphology and the size were visualized by TEM (JEM 2100). The optical properties were measured by Photoluminescence spectra (NIR512).

III. Result and Discussion

The XRD spectrum of the Ga-Co-ZnSe NPs is shown in Fig. 1. Two diffraction peaks in the pattern can be indexed to the (220) and (311) lattice planes of the ZnSe (JCPDS37-1463). The peak of (510) corresponded to Ga (JCPDS 43-1012). The diffraction peaks of all NPs are consistent with target [13]. With the increase of Ga content from 10% to 50%, the peak of (510) increases gradually, which indicates that the absorption of Ga by ZnSe is limited. There is no information about Co in the pattern, which also means that Co has been doped into ZnSe and substituted some of the Zn atoms [14]. The crystal structure is confirmed by the patterns of NPs with different concentration because all the result shows the sharp peak. Therefore, the NPs with same crystal structure of target are confirmed. In fact, the structure of the materials has a significant influence by plasma plume in the process of preparation. By changing the pulse deposition time and energy density of the pulse laser, the surface of the target is ablated at high temperature, which makes the temperature of the target spot rapidly increase to the vaporization state, so that the material atoms absorbed enough energy to sputter it from the surface. Therefore, the harder the material is, the smaller the plasma plume. But, in condition of high temperature and pressure, more and more active gas molecules will collide with the plasma. The obvious boundary phenomenon was washed away. The area of plasma plume is enlarged, and the impact force is weakened, which has an effect on the growth of thin films.

The Raman spectra of the NPs are shown in Fig. 2. The peaks at 168, 171 and 181 cm^{-1} are considered as the phonon vibration of Co-S in short-wave Raman drift region [15], [16]. However, the peaks at 238 and 248 cm^{-1} demonstrate that transitions in multi-level orbits occur more frequently at the closely concentration of Co and Ga. Because the peak is not found at 50%-10%-40% concentration, we believe that the peaks at 238 and 248 cm^{-1} belong to the vibration information of Co-Ga. Raman peaks at 332, 340 and 360 cm^{-1} in the are attributed to longitudinal optical (LO) modes [16], [17]. Besides, the peaks at 482, 487 and 600 cm^{-1} are gradually diminished with the decreasing of Ga concentration. Thus, these peaks can be explained by the characteristic peaks of the phonon vibration of the Ga or Ga-O bones [18], [19]. The peak at 1365 cm^{-1} is due to the quartz glass substrates. Raman spectroscopy supplements the information not stated in the XRD spectrum. The bond about Co-S confirmed that the Co has been doped in the ZnS, and replaced the Zn+.

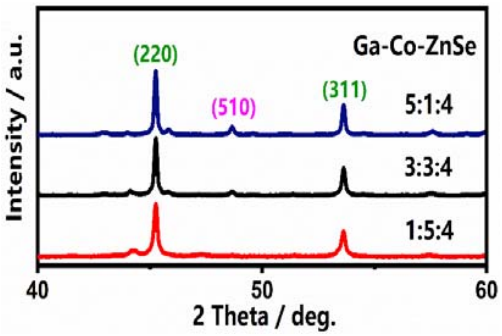

Fig. 1 The XRD spectrum of the Ga-Co-ZnSe NP

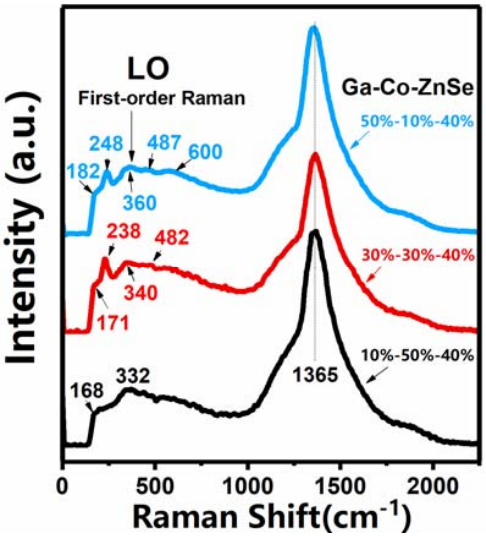

Fig. 2 Raman spectra of the Ga-Co-ZnSe ceramic bulks

The TEM images of circular-shaped multi-doping NPs are shown in Fig. 3. In the experiment, all NPs are circular in shape at 500 mW laser power. Fig. 3 (a) shows the regular NPs at 50 nm scale, which illustrates that we have solved the cluster phenomenon by the PLA. In the scale of 5 nm, the size distribution of NPs ranges from 5 to 7 nm and disperses with each other, which indicates that our preparation method is more uniform. Two lattice planes marked are (220) with 0.364 nm and (311) with 0.296 nm, which proves the crystal structure in the particles, as seen in Fig. 3 (c). In fact, materials with magnetic elements such as Co or Fe, in general, are not allowed to detect TEM or SEM. There are two main difficulties in this problem. First, the magnetic particles are adsorbed on the eyepiece by the strong magnetic field in the electron microscope, causing pollution. Second, after receiving TEM strong magnetic field interference, the magnetic particles will have a large number of clusters, which makes the characterization fail. In this test, we use resin polymer

embedding with ultra-thin slices, and drop one drop at a time to control the concentration. However, this work is of great risk and difficulty.

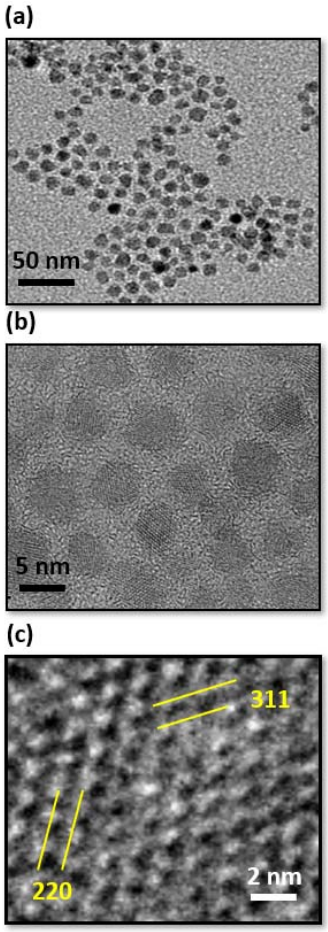

Fig. 3 TEM image of the Ga-Co-ZnS nanomaterials: (a) 50 nm, (b) 5 nm, (c) Lattice image of shuttle-shaped NP

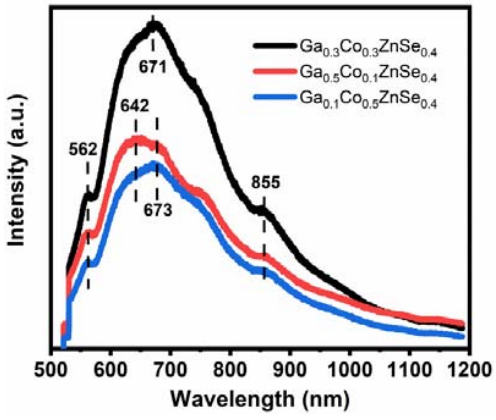

Fig. 4 Room temperature photoluminescence (PL) spectra of Ga-Co-ZnS NP with different concentration

Fig. 4 represents the PL spectra of Ga-Co-ZnS NPs with different shape and concentration. The peak at 562 nm is found in the all of three concentrations, which is attributed to the energy level exchange between transition metal elements. The peak at 673 nm is detected in the Co-rich concentration ($Ga_{0.1}Co_{0.5}ZnS_{0.4}$). The peak changed from 673 nm to 671 nm with the concentration of Co. Meanwhile, the intensity of the peak 642 nm is the highest in Ga-rich materials. The peak strength decreases greatly with the decrease of Ga content. These changes are consistent with the elemental concentration and Raman results, which show the success of doping. What's important, more peaks and highest intensity are reflected in the $Ga_{0.3}Co_{0.3}ZnS_{0.4}$, which can be attributed to an increase in energy levels caused by closer concentrations of Co and Ga. Besides, the peak at 562 nm is found in the all of three concentrations due to the infrared properties of the Co and ZnSe. All the shift of PL peaks is consistent with the shift of the Raman vibration information, which confirms that the PL emission does change with the structure and different composition ratio of the material at room temperature.

IV. Conclusion

The $Ga_xCo_{1-x}ZnS_{0.4}$ (x= 0.1, 0.3, 0.5) NPs were fabricated via PLA technology. Crystal structure of all nanoparticles was confirmed by XRD. Raman spectrum displayed bonding vibration information of multi-doped elements. The morphology of the NPs is characterized by TEM indicating the availability of our method. More abundant energy level and better optical properties were suggested by PL spectra, particularly in concentration of 30%-30%-40%. In conclusion, we have provided an effective method for preparing NPs. The size and shape of the particles are relatively uniform. Cluster problem has been effectively solved. Finally, a kind of multi-doped composite nanomaterials with multi-level orbits is achieved in this work.

Acknowledgment

This work was supported by the National Natural Science Foundation of China under Youth Science Foundation Project (NSFC-61805005).

References

[1] I. G. Theodorou, Q.F. Jiang, L. Malms, X.Y. Xie, R. C. Coombes, E. O. Aboagye, A. E. Porter, M. P. Ryana and F. Xie. Fluorescence enhancement from single gold nanostars: towards ultra-bright emission in the first and second near-infrared biological windows (J). Nanoscale, 10, 15799 (2018).

[2] C.G. Wang, A.A. Levin, J. Karel, S. Fabbrici, J.F. Qian, C.E. ViolBarbosa, S. Ouardi, F. Albertini, W. Schnelle, J. Rohlicek, G.H. Fecher and C. Felser. Size-dependent structural and magnetic properties of chemically synthesized Co-Ni-Ga nanoparticles (J). Nano Res, 10(10):3421-3433 (2017).

[3] Jappor HR, Habeeb MA Optical properties of two-dimensional GaS and Ga Semonolayers (J). Physica E, 101:251-255 (2018).

[4] M. Akie, T. Fujisawa, T. Sato, M. Arai, K. Saitoh. GeSn/SiGeSn Multiple-Quantum-Well Electroabsorption Modulator with Taper Coupler for Mid-Infrared Ge-on-Si Platform (J). IEEE J Sel Top Quant, 24(6):2827673 (2018).

[5] S. Cao, J.J. Zheng, C.C. Dai, L. Wang, C.M. Li, W.Y. Yang, M.H. Shang, Doping concentration-dependent photoluminescence properties of Mn-doped Zn-In-S quantum dots (J). J Mater Sci, 53, (2), 1286-1296 2018.

[6] Ou K, Wang SW, Huang ML, Zhang YW, Wang Y, Duan XX, Yi LXInfluence of thickness and annealing on photoluminescence of nanostructured ZnSe/ZnS multilayer thin films prepared by electron beam evaporation (J). J Lumin, 199:34-38 (2018).
[7] X.F. Xu, W. Wang, D.L. Liu, D.D. Hu, T. Wu, X.H. Bu, P.Y Feng. Pushing up the Size Limit of Metal Chalcogenide Supertetrahedral Nanocluster (J). J Am Chem Soc, 140(3), 888-891 (2018).
[8] M. Mehrabi, P. Parvin, A. Reyhani and S.Z. Mortazavi, Hybrid laser ablation and chemical reduction to synthesize Ni/Pd nanoparticles decorated multi-wall carbon nanotubes for effective enhancement of hydrogen storage (J). Int J Hydrogen Energ, 43, 12211-12221 (2018).
[9] Rames. M., O.Heczko, A.Sozinov, K.Ullakko, L.Straka, Magnetic properties of Ni-Mn-Ga-Co-Cu tetragonal martensites exhibiting magnetic shape memory effect (J). Scripta Materialia, 142, 61-65, (2017).
[10] S. Cao, J.J. Zheng, C.C. Dai, L. Wang, C.M. Li, W.Y. Yang, M.H. Shang, Doping concentration-dependent photoluminescence properties of Mn-doped Zn-In-S quantum dots (J). Journal of Materials Science, 53, (2), 1286-1296.
[11] Ming Luo. Energy transfer between Co2+ and Fe2+ ions in diffusion-doped ZnSe (J). Journal of Applied Physics, 2005, 98(083507): 1-5.
[12] T. Tanaka, N. Ito, M. Akutsu, K. Chikamatsu, S. Takado and K. Nakahara. Extraction of net acceptor type trap density in semi-insulating GaN layers grown on Si substrate by DC I-V measurement (J). Phys. Status Solidi A, 214(8):1600925 (2017).
[13] Y. Pan, L. Wang, S.F. Li, DW. Gao and X.W. Han, Preparation and characterization of Co and Ga2O3-codoped ZnS and ZnSe bulk ceramics (J). RSC Adv, 7(80), 50928 - 50934 (2017).
[14] Y. Pan, L. Wang, S.F. Li, DW. Gao and X.W. Han, H.H. Yan, Investigation on the (Co, Ga2O3) co-doped ZnSe chalcogenide composite semiconductor thin films fabricated using PLD (J). RSC Adv, 8, 14916 -14924 (2018).
[15] D. Dohy, G. Lucazeau. Valence force-field and Raman-spectra beta -Ga2O3 (J). J Mol Struct, 79(1-4): 419-422 (1998).
[16] M. Choi and J. Son, "Doping-induced bandgap tuning of alpha-Ga2O3 for ultraviolet lighting," Curr Appl Phys 17(5), 713–716 (2017).
[17] O. Brafman, S.S. Mitra, Phys. Rev. 931, 171 (1968).
[18] W.G. Nilsen, Phys. Rev. 838, 182 (1969).
[19] Y.H. Gao, Y. Bando, T. Sato, "Synthesis, Raman scattering and defects of β-Ga2O3 nanorods," Appl. Phys. Lett. 81(12), 2267–22269 (2002).